# The Contact Pressure Analysis of Different Load and Diameter Ratio on Hemispherical Contact: Biomechanical Perspectives

*M. Danny Pratama Lamura, Cucu Bachtiar Achmad, Muhammad Imam Ammarullah, Mohamad Izzur Maula, Farhan Ali Husaini, Athanasius Priharyoto Bayuseno, J. Jamari**
*Department of Mechanical Engineering, Faculty of Engineering, Diponegoro University, Tembalang, Semarang 50275, Central Java, INDONESIA*
**j.jamari@gmail.com*

*Taufiq Hidayat*
*Department of Mechanical Engineering, Faculty of Engineering, Universitas Muria Kudus, Kudus 59352, Central Java, INDONESIA*

ABSTRACT

*Contact mechanics is pivotal in understanding interactions between surfaces, particularly in biological contexts and the human body. When surfaces come into contact, the roughness represented by microscopic peaks called asperities becomes crucial. In this study, spherical contact modeling is explored, which is an extensively researched area in both engineering and biomechanics. By examining hemispherical contact systems, valuable insights into their biomechanical response are gained. Specifically, the investigation focuses on how geometric variations and applied loads impact contact pressure using finite element analysis. The model comprises two hemispheres with varying diameter ratios. The results show higher diameter ratios increase maximum contact pressure and expand the pressure contour distribution. While M1 shows similar pressure distribution in both hemispheres under additional load, M2 and M3 exhibit a broader distribution in the bottom hemisphere compared to the upper. Consequently, lower diameter ratios emerge as safer design choices, whereas higher ratios require careful load management to prevent failure.*

ISSN 1823-5514, eISSN 2550-164X

https://doi.org/10.24191/jmeche.v13i1.3757

Received for review: 2024-04-01
Accepted for publication: 2024-07-04
Published: 2024-11-15

**Keywords:** *Contact Mechanics; Hemisphere; Diameter Ratio; Biomechanical; Contact Pressure*

## Introduction

Contact mechanics is crucial in understanding the interaction between two different surfaces, particularly in biology and the human body system [1]. Surface studies help identify the characteristics of contacting surfaces, such as roughness [2], smoothness, and the presence of lubricating layers. This information influences contact mechanics analysis and can be used to optimize system performance. From the biomechanical perspective, contact mechanics involves understanding how forces, deformations, and pressures are distributed when two surfaces come into contact [3]. A good understanding of contact mechanics is highly relevant in various biomechanical applications, such as prosthetic design and evaluation [4], joint motion understanding [5]-[7], and implant-bone interaction [8].

The analysis and application of spherical contact modeling have been topics for established investigation, with ongoing research and development initiatives persisting in this field to the present day. This model has broad applications in engineering and biomechanics [9]. Through accurate modeling, researchers can gain valuable insights into the biomechanical response of hemispherical contact systems. This has significant implications for comfort, stability, and energy efficiency. For instance, Ambrosio and Silva [9] described kinematic joints for biomechanical models with spherical types, such as the back (twelfth thoracic and first lumbar vertebrae), Torso-Neck (seventh cervical and first thoracic vertebrae), shoulder, and hip joint. From an engineering perspective, it is essential to simplify the analysis. In biomechanics, a simplified model is used to reduce the computation time. The simplified model in spherical contact is frequently analyzed, as shown in Figure 1. For example, the hip joint using ball-on-socket analysis was reported by [4], and total shoulder arthroplasty using the spherical humeral head with a glenoid surface was reported by [10]. The study by [11] investigated using a rigid sphere interacting with a deformable plane as a simplified model for human skin. In the other study, the sphere is used for impactor or indentation as an impactor of teeth [12] and an indentation of the human cervix [13]. The centre axis for bending and rotating the knee joint using a spherical centre axis was reported by [14] and [15]. Then, the contact between the two hemispheres was applied to the articular joints or synovial joints [16]. However, the contact between the two hemispheres was equal to that of the sphere against rigid flat in the deformation [17].

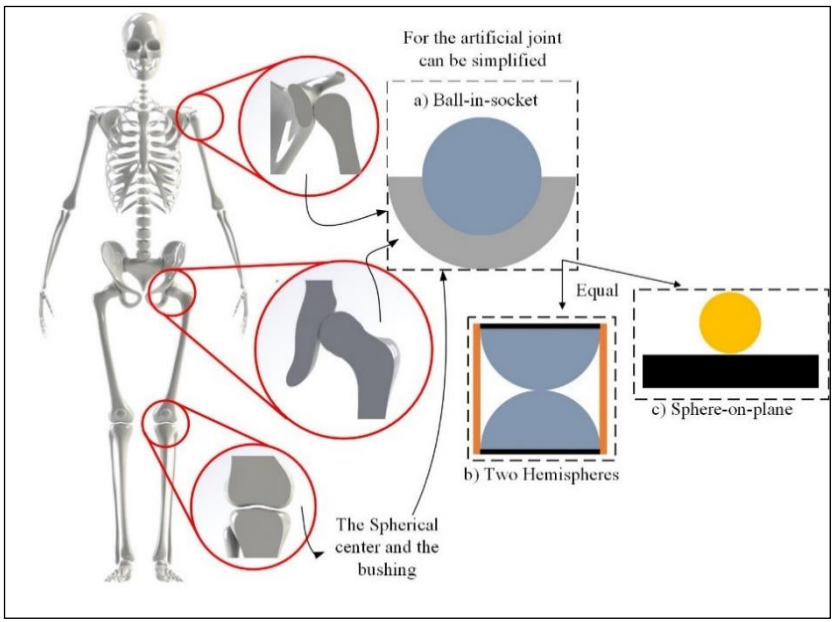


Figure 1: Type of spherical contact; a) ball in the socket, b) two deformable hemispheres, and c) sphere on plane

Analysis of displacement, von Mises stress, and contact pressure are crucial in design or material selection. All three factors must be considered to ensure the designed object has a longer service lifetime. In biomechanical research, contact pressure analysis is crucial as it aids in understanding pressure distribution. Pressure distribution can assist in designing comfortable and safe tools or objects. This is because contact pressure can determine the pain threshold in biomechanics [18]. According to Mak et al. [19], common pressure threshold measurements include minimum pressure to cause pain or discomfort and pressure tolerance, the maximum pressure a person can tolerate without excessive effort. Predicting biomechanical responses, improving designs, performance, and model validation become possible in biomechanical research with hemispherical contact. For instance, contact pressure analysis is essential for total hip joints as it correlates with linear and volumetric wear [20]-[21]. Estimating the contact area of artificial hip joints during daily activities is essential in predicting joint degeneration mechanisms and prosthetic implant wear, providing a biomechanical basis for preoperative planning and postoperative rehabilitation [22]. Pressure distribution analysis in feet can be influenced by shoe design and serves as a guide in ergonomic shoe design [23]. Willinger et al. [24] stated that the maximum pressure caused by Medial Meniscus Extrusion (MME) must be controlled to reduce the

development of osteoarthritis. Kitamura et al. [7] reported that changes in posture in physiological pelvic tilt affect joint contact pressure in the hip. Monta and Ghosh [25] reported that implant orientations increased contact pressure from 4.2 MPa at 5º to 7 MPa at 10º. In contrast, implant material had an insignificant effect.

Hemispherical or spherical contact analysis is also conducted on human skin, such as Adams et al. [11] conducting in vivo friction analysis on dry, wet, and moist human skin using smooth glass and polypropylene spherically tipped probes. The results showed that the prediction of the adhesive friction coefficient did not depend on the normal load for spherically tipped probes due to the roughness of the skin surface topography. Friction force depended more on the shear strength of the skin interface, which decreased with the presence of moisture, even in dry conditions. Adams et al. [11] align with a previous study [26], which stated that the friction coefficient does not have a significant influence on the two-hemisphere model under full plastic contact conditions. Furthermore, the mechanical properties analysis in human skin analysis assumes elasticity in many cases. Thus, the Hertz contact theory is used [27]. The study of contact pressure can be conducted to assess the possibility of discomfort and pain in a design that requires interaction with the skin.

Several researchers have conducted contact pressure analysis in various cases. Gil-Agudo et al. [28] analyzed pressure distribution and contact surface in the user interface and wheelchair cushion for individuals with spinal cord injuries. The research showed that dual-compartment air cushions provided the best pressure distribution and a larger contact surface. Additionally, Buchler et al. [29] developed a finite element model to analyze the humeral head shape's influence on scapula stress distribution. This study compared normal shoulders with osteoarthritic shoulders and showed that posterior translation occurred during rotation in osteoarthritic shoulders, which was associated with increased contact pressure. Furthermore, Park et al. [30] developed a new method to obtain contact pressure distribution in knee and ankle joints using finite element analysis, muscle forces, and ground reaction forces as load conditions. This method allowed modeling contact pressure distribution on the tibial plateau and talus cartilage during the gait cycle.

On the other hand, Sukpat et al. [31] investigated wear due to impact on Steel AISI 4140 using a combination of computational techniques and empirical data. They developed a 2D finite element model to analyze contact conditions and validated predictions with empirical data. However, this study did not consider contact geometry variations with wear progression, which could affect contact pressure estimates.

This study examined the investigations of geometric and load variations on contact pressure using the finite element method. Geometric variations in this study involve hemisphere diameter ratios. The contact phenomenon has been discussed comprehensively, and its application is from the biomechanical perspective.

## Materials and Method

### Geometric parameters and material properties

The model used in this study consists of two hemispheres with varying diameter ratios, as shown in Figure 2.

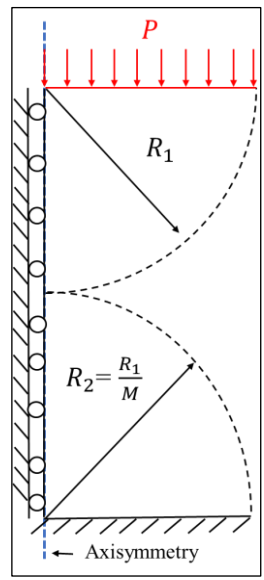


Figure 2: The schematic of M1 model

It can be described that $M$ is the diameter ratio while $R_1$ and $R_2$ are the radius of each hemisphere. Hemisphere 1 has a constant value of 17.5 mm. The diameter ratio is the ratio of the diameter of hemisphere 1 to the diameter of hemisphere 2, as given in Equation (1), and Table 1 shows the details of the sizing for the model setup. The diameter ratio in this study ranges from 1 to 3 times. The selection models caused the previous study [26] to have a very good agreement in the ratio diameter 1 to 3.

$$M = \frac{R_1}{R_2} \tag{1}$$

The material used in this study is brass with elastic-perfectly plastic material properties, which its material properties are shown in Table 2. The materials assume isotropic. Brass material has been used for medical industry applications such as dental equipment [32], diagnostic devices [33], and medical instruments [34].

Table 1: The model setup

| Model | Radius (mm) | |
|---|---|---|
| | **The upper hemisphere ($R_1$)** | **The bottom hemisphere ($R_2$)** |
| M1 | 17.5 | 17.5 |
| M2 | 17.5 | 8.75 |
| M3 | 17.5 | 5.83 |

Table 2: The material properties of Brass

| Property | Value | Unit |
|---|---|---|
| Elastic modulus | 96 | GPa |
| Poisson ratio | 0.34 | - |
| Yield strength | 310 | MPa |

## Finite element method

The finite element model is discretized using ABAQUS CAE 2020 software. The elements used in this study are CAX4R elements. A 2D axisymmetric model and local meshing are used to save computational costs, with a local mesh radius of $R'$. Equation (2) shows the calculation of the value of $R'$.

$$R' = \left(\frac{1}{R_1} + \frac{1}{R_2}\right)^{-1} \tag{2}$$

The boundary condition in this study is fixed in all directions in the base of the bottom hemispheres. The type of contact used is static general with surface-to-surface interaction. In this case, both materials have the same hardness and mesh size. The choice of the master surface is based on the harder material or coarser meshing [35]. Therefore, the master surface chosen is hemisphere two due to its smaller diameter in higher diameter ratio cases. Loading is applied using a point load of 500 N, 1000 N, 2500 N, and 8000 N with coupling constraints options to distribute the forces in the surfaces, as shown in Figure 2. The contact property uses pressure-overclosure hard contact and constraint enforcement methods using the augmented Lagrange algorithm. This caused the augmented Lagrange to be suitable for frictionless contact [36], the normal material behavior contact problem [37]-[38], the plasticity problem [39], and to avoid the convergence problem [40]. The contact of this study was assumed to be frictionless.

## Results

Simulations are performed repeatedly to obtain an ideal mesh, referred to as a mesh convergence study. A finer mesh incurs higher computational costs, while a coarser mesh provides less accurate results [41]. The ideal mesh does not affect simulation results. In this case, the perfect mesh is chosen for each model. In M1, 47040 elements were chosen; in M2, 26880 elements were chosen; and in M3, 14080 elements were chosen. M1 has a difference of 0.01%, M2 has a difference of 0.006%, and M3 has a difference of 0.0017%. After finding the ideal mesh, a comparative study is conducted with previous researchers to determine the validity and readiness of the simulation for analysis according to the observed case. After finding the ideal mesh, a comparative study is conducted with previous researchers to determine the validity and readiness of the simulation for analysis according to the observed case.

Comparative studies are conducted to ensure the finite element model's validity. Contact between a ball and a flat rigid surface is equivalent to the contact between two hemispheres [26]. The relationship between dimensionless displacement ($\omega^*$) and dimensionless load ($P^*$) is shown in Figure 3. The dimensionless displacement value is $\omega$ divided by the critical displacement ($\omega_c$), while $P^*$ is $P$ divided by the critical load ($\omega_c$). The critical displacement and load values in this study are the critical values from the equations in [42]. For detailed information on dimensionless load and displacement, refer to [17]. Comparative studies are performed with the Kogut and Etsion (KE) and Jackson and Green (JG) contact models against the present study models M1-M3. The results show very good agreement between the present study and the KE contact model, with less than 4.5% differences (see Table 3). Thus, this simulation can be considered valid.

Figure 3 shows that increasing the diameter ratio leads to higher dimensionless displacement and dimensionless load at the same load. This is due to the decrease in $R'$ with increasing diameter ratio. The load-bearing capacity of the lower diameter ratio is impacted more significantly at lower loads compared to the higher diameter ratio. The lines of the JG and KE equations hold only for $\omega^* \leq 110$, and when values exceed 110, the results are validated according to Lamura et al. [26]. The load variation (500 N, 1000 N, 2500 N, 5000 N, and 8000 N) was chosen based on the regime contact regime outlined by Equations (7) and (8) in the KE contact model [43]. Where in the M1, the 500 N load was near the dimensionless interference $\omega^* = 6$, and the 8000 N is near the $\omega^* = 110$. The $\omega^*$ will be increased in the same load for a higher diameter ratio. This increase caused the higher diameter ratio to have a smaller $\omega_c$ than the lower diameter ratio. The far of $\omega^*$ from 110, the contact is very deep in the fully plastic contact. The details of differences and the value of $\omega^*$ are shown in Table 3.

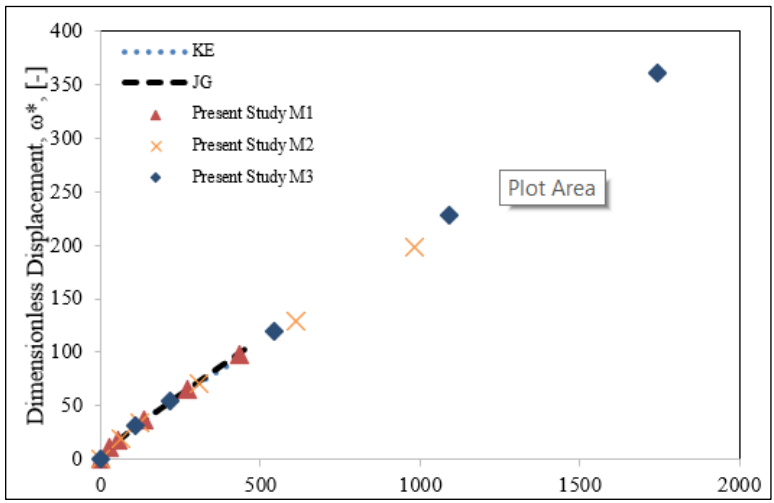


Figure 3: Comparison of the present study with analytical approach from contact model KE and JG

Table 3: Comparison results between KE and M1

| P (N) | P* | $\omega^*$ | | Deviation (%) |
|---|---|---|---|---|
| | | KE | Present Study | |
| | | M1 | | |
| 500 | 27.24 | 10.49 | 10.62 | 1.23 |
| 1000 | 54.48 | 18.16 | 17.94 | 1.23 |
| 2500 | 136.21 | 37.51 | 37.16 | 0.93 |
| 5000 | 272.42 | 64.93 | 65.14 | 0.33 |
| 8000 | 435.87 | 94.20 | 98.29 | 4.16 |
| | | M2 | | |
| 500 | 61.29 | 19.93 | 19.64 | 1.48 |
| 1000 | 122.59 | 34.50 | 33.74 | 2.28 |
| 2500 | 306.47 | 71.28 | 71.30 | 0.03 |
| 5000 | 612.94 | 123.39 | 129.27 | - |
| 8000 | 980.71 | 179.02 | 198.12 | - |
| | | M3 | | |
| 500 | 108.97 | 31.43 | 30.89 | 1.75 |
| 1000 | 217.94 | 54.41 | 54.23 | 0.34 |
| 2500 | 544.84 | 112.40 | 119.66 | - |
| 5000 | 1089.68 | 194.59 | 227.56 | - |
| 8000 | 1743.49 | 282.32 | 360.57 | - |

The subsequent increase in load corresponds to an increase in contact pressure. Increasing the diameter ratio also leads to increased contact pressure, as shown in Figure 3. At a load of 500 N, the maximum contact pressure values are M1 (747.72 MPa), M2 (770.20 MPa), and M3 (815.66 MPa). Furthermore, at a load of 8000 N, the maximum contact pressure values are M1 (877.55 MPa), M2 (919.91 MPa), and M3 (999.55 MPa). The increase in maximum contact pressure at lower loads is significantly higher than the increase at higher loads. This is in line with the mean contact pressure report by [43], which shows that higher loads or more distant strain levels result in a reduction in the increase of contact pressure.

Figure 4 illustrates the relationship between maximum contact pressure and load. The contour of contact pressure is shown in Figure 5. At loads of 500 N and 1000 N, the contour distribution of contact pressure is the same between the upper and lower hemispheres in all diameter ratios. Increasing the diameter ratio leads to an expansion of the maximum pressure area located beneath the contact area. When increasing the load from 500 N to 8000 N, the distribution of contact pressure widens, and differences in the spread of contact pressure become apparent. In M1, the widening of the contact pressure remains uniform between the upper and lower hemispheres. In contrast, in M2 and M3, at a load of 2500 N, differences start to appear, with the widening of contact pressure being greater in the lower hemisphere compared to the upper hemisphere. This indicates that the lower hemisphere experiences a higher impact, consistent with the findings of [26]. Therefore, designing with a diameter ratio of 1 is safer than higher diameter ratios for higher loads. Conversely, lower loads are recommended for higher diameter ratios to avoid failure.

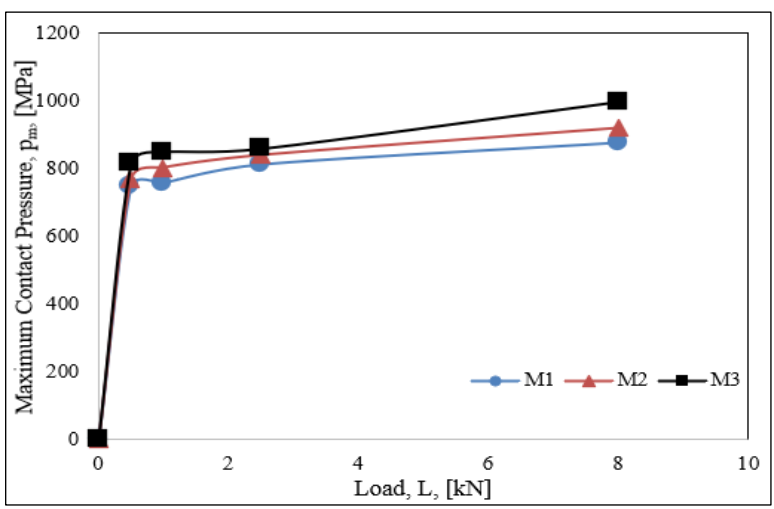


Figure 4: Maximum contact pressure against load

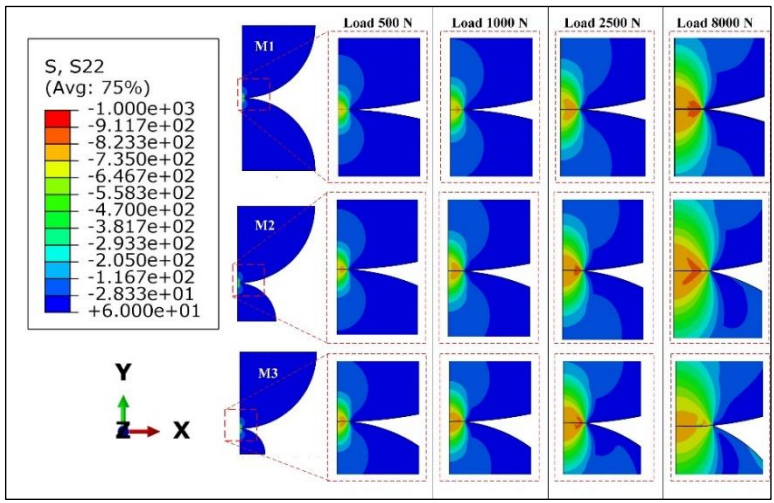


Figure 5: The contour of contact pressure

Figure 6 shows the contour and the contact pressure distributions in the load 5000 N. The load 5000 N has been selected to be a more detailed result phenomenon for the different diameter ratio effect. This selection is because the variation of load shows a similar phenomenon. Figure 6(a) shows the wider contour of contact pressure when the diameter ratio increases. Figure 6(b) can be seen for the upper and the bottom hemispheres; increasing the diameter ratio can increase the radial distance of contact pressure to a high value. The radial distance of 2 mm to 17.5 mm depicts the increasing diameter of the ratio and the increased contact pressure.

Based on the report by [44], fully plastic contact has almost flattened pressure, and further increases in the contact force only result in an enlargement of the contact area with no apparent increase in the maximum contact pressure. The contact pressure distributions in M1 are identically in the upper and bottom hemispheres. The identical contact pressure distributions are in line with [45] reported. However, the increase in the diameter ratio will make the load higher impact on the bottom hemisphere and become the different contact pressure distribution between the upper hemisphere and the bottom hemisphere. This phenomenon occurs when the bottom hemisphere has a different regime from the upper hemisphere.

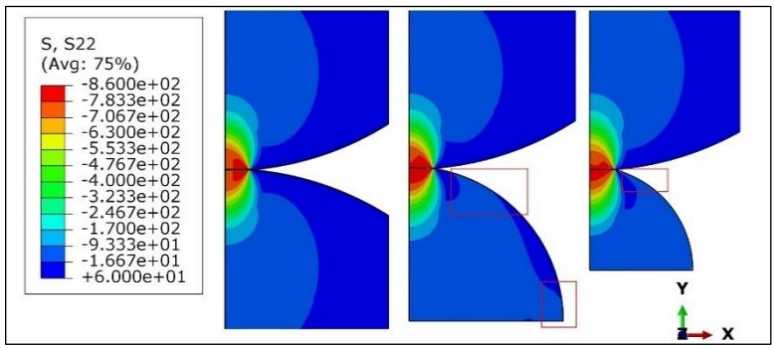


(a)

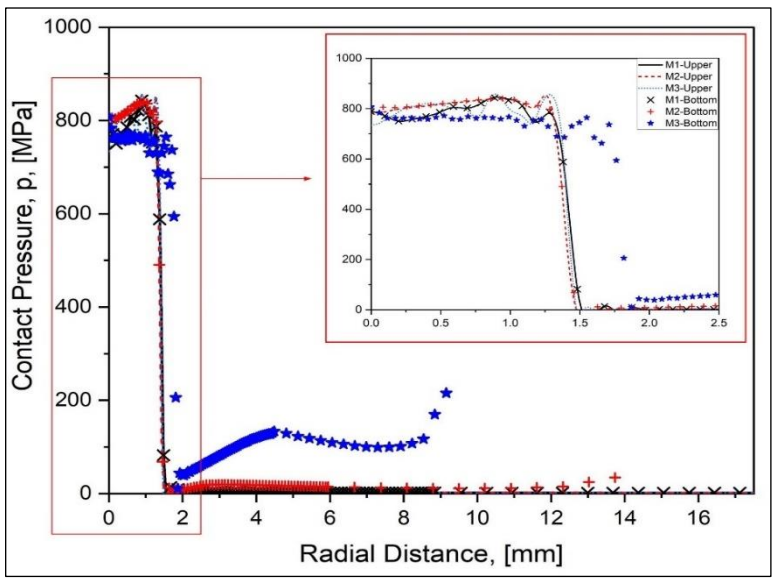


(b)

Figure 6: (a) The contour of contact pressure in the load 5000 N, (b) The contact pressure distribution against radial distance

## Discussion

The spherical contact is widely used for analysis in the field of biomechanics. Several studies have reported biomechanics analysis as a macro scale and spherical contact as a part of the analysis. For example, Heb and Forsbach [4] have developed analytical models for total hip arthroplasty as an application

of spherical contact. Urribarrí et al. [46] have modeled a fingertip (as a sphere) where the contact area was analyzed. Adams et al. [11] used the rolling contact concept with the Tabor-Eldredge tribometer to observe a spherical tip in motion across the inner forearm's surface while a load was applied in the steady normal contact. Kuilenburg et al. [27] have analyzed the effective elastic modulus with the simplified contact model of the sphere and the skin (modeled as a flat deformable). So, analyzing spherical contact is crucial to understanding mechanical behavior, especially from the perspective of biomechanics.

Despite the extensive research on contact area analysis and the application of spherical contact for biomechanics, the study of contact pressure and variations in geometry size remains relatively limited. This is crucial, as surfaces exhibit roughness, with individual asperities often modeled as spheres for simplification [47], potentially leading to significant variations in contact behavior.

The finite element study initiated with a mesh convergence analysis, which is crucial for ensuring the accuracy of finite element simulations. By selecting an ideal mesh size for each model (M1, M2, and M3), the researchers achieve a balance between computational cost and accuracy. Subsequently, the results from mesh convergence analysis must be compared with the experimental study from other research. The study compares the results obtained from the present models (M1-M3) with established contact models (KE and JG), where the present study has been validated, and the model has been prepared for subsequent analysis.

The results highlight the influence of the diameter ratio on dimensionless displacement, dimensionless load, and maximum contact pressure. Increasing the diameter ratio leads to higher dimensionless displacement and dimensionless load at the same load, primarily due to decreased effective radius. Moreover, higher diameter ratios increase contact pressure, particularly at lower loads. This understanding is crucial for designing components with varying diameter ratios to withstand different loads effectively.

In the analysis of a hip joint, an increase in contact pressure along with wear rate [48]. If this wear is not addressed by improving the design or using stronger materials under higher pressure, the service life of the hip joint will be shortened. In addition to the increase in maximum contact pressure, Figure 4 also shows an increase in the distribution of contact pressure. The first areas to experience failure are those with the highest contact pressure, indicated by the red color. The red color appears in the corner, signifying potential cracks in that corner area. Smaller diameter ratios have a higher potential for failure. This aligns with the von Mises stress and deformation analysis [26], and equivalent plastic strain (PEEQ) analysis [17] results as well as the current study.

The findings of this study indicate that increasing the diameter ratio increases the maximum contact pressure. Therefore, smaller diameter ratios are recommended for design. This is because each material has a tolerance limit. In the biomechanical context, the observed tolerance limit, according to [18] is the maximum contact pressure. In this case, the maximum contact pressure is concentrated in the corner of the contact area. Plastic contact occurs, making the deformation of the object irreversible. Most biomechanical analyses assume pure elasticity [27]. Thus, it is interesting to analyze this in biomechanical models such as the knee, skin, shoulder, etc., with full plastic contact.

The limitations of this study include, first, the use of material with elastic-perfectly plastic properties. It is essential to consider strain hardening when using metal materials because plastic deformation results in strain hardening, causing an increase in the force required to change the shape of the object [49]. Second, the model used in this study is a simple 2D axisymmetric model, so the complex model includes reconstruction from the human bone or the 3D implant geometry. Third, the material used is brass, which has the same hardness. It is essential to consider other materials with the same or different hardness, such as hard-on-soft and soft-on-hard. Fourth, the simulation in this study has a normal load with static contact without repeated load and tangential load. In engineering and biomechanics problems, the contact will be repeated for a long time [50]-[52]. These limitations will be addressed in future research.

## Conclusion

This study investigated the effect of geometry and load variation on contact pressure using FEA, focusing on biomedical applications. The results showed that an increased diameter ratio leads to higher maximum contact pressure and a wider distribution of contact pressure contours. For identical geometries, contact pressure distribution remained consistent and safer compared to different-sized geometries, particularly in hemispherical contacts. Material properties significantly influence contact pressure and deformation behavior. Future research should explore materials with implant materials with elastic-plastic materials, the geometry more complex, such as reconstruction from the human bone or the 3D implant geometry.

## Contributions of Authors

The authors confirm the equal contribution in each part of this work. All authors reviewed and approved the final version of this work.

## Funding

This work was supported by the Ministry of Education, Culture, Research and Technology of the Republic of Indonesia through a scholarship of the Master Education Program Leading to Doctoral Degree for Excellent Graduates (PMDSU) [grant number: 345-44/UN7.D2/PP/V/2024].

## Conflict of Interests

All authors declare that they have no conflicts of interest.

## Acknowledgment

All authors thank all participants for joining this study and cooperating.

## References

[1] S. A. Rodeo, F. Monibi, B. Dehghani, and S. Maher, "Biological and mechanical predictors of meniscus function: Basic science to clinical translation," *Journal of Orthopaedic Research*, vol. 38, no. 5, pp. 937–945, 2020. doi: 10.1002/jor.24552

[2] J. Jamari, M. B. de Rooij, and D. J. Schipper, "Plastic deterministic contact of rough surfaces," *Journal of Tribology*, vol. 129, no. 4, pp. 957–962, 2007. doi: 10.1115/1.2768618

[3] J. C. Küpper, P. Zandiyeh, and J. L. Ronsky, "Empirical joint contact mechanics: A comprehensive review," *Proceedings of the Institution of Mechanical Engineers Part H Journal of Engineering in Medicine*, vol. 237, no. 2, pp. 147–162, 2023. doi: 10.1177/09544119221137397

[4] M. Heß and F. Forsbach, "An analytical model for almost conformal spherical contact problems: Application to total hip arthroplasty with uhmwpe liner", *Applied Science*, vol. 11, no. 23, 2021. doi: 10.3390/app112311170

[5] J. H. Calhoun, F. Li, B. R. Ledbetter, and S. F. Viegas, "A comprehensive study of pressure distribution in the ankle joint with inversion and eversion", *Foot & Ankle International*, vol. 15, no. 3, pp. 125–133, 1994. doi: 10.1177/107110079401500307

[6] E. Genda, N. Iwasaki, G. Li, B. A. MacWilliams, P. J. Barrance, and E. Y. S. Chao, "Normal hip joint contact pressure distribution in single-leg standing-effect of gender and anatomic parameters," *Journal of Biomechanics*, vol. 34, no. 7, pp. 895–905, 2001. doi: 10.1016/S0021-

9290(01)00041-0

[7] K. Kitamura, M. Fujii, S. Ikemura, S. Hamai, G. Motomura, and Y. Nakashima, "Does patient-specific functional pelvic tilt affect joint contact pressure in hip dysplasia? A finite-element analysis study", *Clinial Orthopaedics and Related Research*, vol. 479, no. 8, pp. 1712–1724, 2021. doi: 10.1097/CORR.0000000000001737

[8] Y. Wang, Q. Tan, F. Pu, D. Boone, and M. Zhang, "A review of the application of additive manufacturing in prosthetic and orthotic clinics from a biomechanical perspective", *Engineering*, vol. 6, no. 11, pp. 1258–1266, 2020. doi: 10.1016/j.eng.2020.07.019

[9] J. Ambrósio and M. Silva, "Multibody dynamics approaches for biomechanical modeling in human impact applications", *Solid Mechanics and its Applications*, vol. 124, pp. 61–80, 2005. doi: 10.1007/1-4020-3796-1_7

[10] L. N. Muench, M. Murpher, B. M. Oei, C. Kia, E. Obopilwe, M. P. Cote, A. Mazzocca, and D. P. Berthold, "Elliptical and spherical heads show similar obligate glenohumeral translation during axial rotation in total shoulder arthroplasty", *BMC Musculoskeletal Disorder*, vol. 24, no. 1, pp. 1–11, 2023. doi: 10.1186/s12891-023-06273-5

[11] M. J. Adams, B. J. Briscoe, and S. A. Johnson, "Friction and lubrication of human skin", *Tribology Letters*, vol. 26, no. 3, pp. 239–253, 2007. doi: 10.1007/s11249-007-9206-0

[12] A. Bachiri, N. Djebbar, B. Boutabout, and B. Serier, "Effect of different impactor designs on biomechanical behavior in the interface bone-implant: A comparative biomechanics study", *Computer Methods and Programs in Biomedicine*, vol. 197, p. 105723, 2020. doi: 10.1016/j.cmpb.2020.105723

[13] L. Shi and K. Myers, "A finite porous-viscoelastic model capturing mechanical behavior of human cervix under multi-step spherical indentation," *Journal of the Mechanical Behavior of Biomedical Materials*, vol. 143, no. 11, pp. 1-11, 2023. doi: 10.1016/j.jmbbm.2023.105875

[14] J. Y. Zhang, J. Wang, D. M. Tian, D. P. Jiang, J. J. Li, and Y. C. Hu, "Spherical center and rotating platform hinged knee prosthesis: Finite-element model establishment, verification and contact analysis", *The Knee*, vol. 27, no. 3, pp. 731–739, 2020. doi: 10.1016/j.knee.2020.04.022

[15] J. yu Zhang, H. ran Zhang, D. mu Tian, F. Wang, H. Zhang, and Y. cheng Hu, "Spherical center axial hinge knee prosthesis causes lower contact stress on tibial insert and bushing compared with biaxial hinge knee prosthesis", *The Knee*, vol. 29, pp. 1–8, 2021. doi: 10.1016/j.knee.2021.01.005

[16] R. B. Martin, D. B. Burr, N. A. Sharkey, and D. P. Fyhrie, Skeletal Tissue Mechanics, 2nd Edition, Springer, 2015. doi: 10.1007/978-1-4939-3002-9

[17] M. Danny Pratama Lamura, M. Imam Ammarullah, T. Hidayat, M. Izzur Maula, J. Jamari, and A. P. Bayuseno, "Diameter ratio and friction coefficient effect on equivalent plastic strain (PEEQ) during contact between two brass solids", *Cogent Engineering*, vol. 10, no. 1, pp. 1-15, 2023. doi: 10.1080/23311916.2023.2218691

[18] C. G. Nim, S. O'Neill, A. G. Geltoft, L. K. Jensen, B. Schiøttz-Christensen, and G. N. Kawchuk, "A cross-sectional analysis of persistent low back pain, using correlations between lumbar stiffness, pressure pain threshold, and heat pain threshold", *Chiropratic & Manual Therapies*, vol. 29, no. 1, pp. 1–11, 2021. doi: 10.1186/s12998-021-00391-4

[19] A. F. T. Mak, M. Zhang, and D. A. Boone, "State-of-the-art research in lower-limb prosthetic biomechanics-socket interface: A review," *Journal of Rehabilitation Research and Development*, vol. 38, no. 2, pp. 161–173, 2001.

[20] F. Liu, Y. He, Z. Gao, and D. Jiao, "Enhanced computational modelling of UHMWPE wear in total hip joint replacements: The role of frictional work and contact pressure", *Wear*, vol. 482–483, pp. 1-8, 2021. doi: 10.1016/j.wear.2021.203985

[21] D. Mazzucco and M. Spector, "Effects of contact area and stress on the volumetric wear of ultrahigh molecular weight polyethylene", *Wear*, vol. 254, no. 5–6, pp. 514–522, 2003. doi: 10.1016/S0043-1648(03)00135-2

[22] H. Yoshida, A. Faust, J. Wilckens, M. Kitagawa, J. Fetto, and E. Y. S. Chao, "Three-dimensional dynamic hip contact area and pressure distribution during activities of daily living," *Journal of Biomechanics*, vol. 39, no. 11, pp. 1996–2004, 2006. doi: 10.1016/j.jbiomech.2005.06.026

[23] S. S. Zulkifli and W. P. Loh, "A state-of-the-art review of foot pressure", *Foot and Ankle Surgery*, vol. 26, no. 1, pp. 25–32, 2020. doi: 10.1016/j.fas.2018.12.005

[24] L. Willinger, J. J. Lang, C. A. V. Deimling, T. Diermeier, W. Petersen, and A> B. Imhoff, "Varus alignment increases medial meniscus extrusion and peak contact pressure: a biomechanical study," *Knee Surgery, Sports Traumatology Arthroscopy*, vol. 28, no. 4, pp. 1092–1098, 2020. doi: 10.1007/s00167-019-05701-1

[25] S. Mondal and R. Ghosh, "Effects of implant orientation and implant material on tibia bone strain, implant–bone micromotion, contact pressure, and wear depth due to total ankle replacement," *Proceedings of the Institution of Mechanical Engineers Part H Journal of Engineering in Medicine*, vol. 233, no. 3, pp. 318–331, 2019. doi: 10.1177/0954411918823811

[26] M. D. P. Lamura, T. Hidayat, M. I. Ammarullah, A. P. Bayuseno, and J. Jamari, "Study of contact mechanics between two brass solids in various diameter ratios and friction coefficient," *Proceedings of the Institution of*

*Mechanical Engineers Part J Journal of Engineering Tribology*, vol. 237, no. 8, pp. 1613-1619, 2023, doi: 10.1177/14657503221144810.

[27] J. Van Kuilenburg, M. A. Masen, and E. Van Der Heide, "Contact modelling of human skin: What value to use for the modulus of elasticity?," *Proceedings of the Institution of Mechanical Engineers Part J Journal of Engineering Tribology*, vol. 227, no. 4, pp. 349–361, 2013. doi: 10.1177/1350650112463307

[28] A. Gil-Agudo, A. De la Peña-González, A. Del Ama-Espinosa, E. Pérez-Rizo, E. Díaz-Domínguez, and A. Sánchez-Ramos, "Comparative study of pressure distribution at the user-cushion interface with different cushions in a population with spinal cord injury", *Clinical Biomechanics*, vol. 24, no. 7, pp. 558–563, 2009. doi: 10.1016/j.clinbiomech.2009.04.006

[29] T. M. Bucher, H. V. Tafreshi, and G. C. Tepper, "Modeling performance of thin fibrous coatings with orthogonally layered nanofibers for improved aerosol filtration", *Powder Technology*, vol. 249, pp. 43–53, 2013. doi: 10.1016/j.powtec.2013.07.023

[30] S. Park, S. Lee, J. Yoon, and S. W. Chae, "Finite element analysis of knee and ankle joint during gait based on motion analysis", *Medical Engineering and Physics*, vol. 63, pp. 33–41, 2019. doi: 10.1016/j.medengphy.2018.11.003

[31] M. Sukpat, J. Kasivitamnuay, and K. Tuchinda, "Computational study of impact wear: Fatigue approach", *Wear*, vol. 528–529, pp. 1-12, 2023. doi: 10.1016/j.wear.2023.204972

[32] O. D. Gonçalves, M. Egito, C. Castro, S. Groisman, M. Basílio, and N. L. da Penha, "About the elemental analysis of dental implants", *Radiation Physics and Chemistry*, vol. 154, pp. 53–57, 2019. doi: 10.1016/j.radphyschem.2018.03.014

[33] D. Nocetti, K. Villalobos, N. Marin, M. Monardes, B. Tapia, M. I. Toledo, C. Villegas, "Radiation dose reduction and image quality evaluation for lateral lumbar spine projection", *Heliyon*, vol. 9, no. 9, pp. 1-9, 2023. doi: 10.1016/j.heliyon.2023.e19509

[34] B. van Straten, B. Tantuo, J. Dankelman, N. H. Sperna Weiland, B. J. Boersma, and T. Horeman, "Reprocessing Zamak laryngoscope blades into new instrument parts; an 'all-in-one' experimental study", *Heliyon*, vol. 8, no. 11, pp. 1-9, 2022. doi: 10.1016/j.heliyon.2022.e11711

[35] R. J. Boulbes, Troubleshooting Finite-Element Modeling with Abaqus: With Application in Structural Engineering Analysis, Springer, 2020. doi: 10.1007/978-3-030-26740-7.

[36] A. R. Khoei, S. O. R. Biabanaki, A. R. Vafa, and S. M. Taheri-Mousavi, "A new computational algorithm for 3D contact modeling of large plastic deformation in powder forming processes", *Computational Materials Science*, vol. 46, no. 1, pp. 203–220, 2009. doi: 10.1016/j.commatsci.2009.02.026

[37] F. Liu and R. I. Borja, "A contact algorithm for frictional crack propagation with the extended finite element method," *International Journal for Numerical Methods in Engineering*, vol. 76, no. 10, pp. 1489–1512, 2008. doi: 10.1002/nme.2376

[38] T. A. Laursen and B. N. Maker, "An augmented Lagrangian quasi-Newton solver for constrained nonlinear finite element applications," *International Journal for Numerical Methods in Engineering*, vol. 38, no. 21, pp. 3571–3590, 1995. doi: 10.1002/nme.1620382103

[39] Q. Peng, Y. Jin, X. Liu, and Y. G. Wei, "Effect of plasticity on the coefficient of restitution of an elastoplastic sphere impacting an elastic plate," *International Journal of Solids and Structures*, vol. 222–223, pp. 1-11, 2021. doi: 10.1016/j.ijsolstr.2021.03.023

[40] M. Cuomo and G. Ventura, "Complementary energy approach to contact problems based on consistent augmented Lagrangian formulation", *Mathematical and Computer Modelling*, vol. 28, no. 4–8, pp. 185–204, 1998. doi: 10.1016/S0895-7177(98)00117-4

[41] W. Zhao and S. Ji, "Mesh convergence behavior and the effect of element integration of a human head injury model", *Annals of Biomedical Engineering*, vol. 47, no. 2, pp. 475–486, 2019. doi: 10.1007/s10439-018-02159-z

[42] R. L. Jackson and I. Green, "A finite element study of elasto-plastic hemispherical contact against a rigid flat," *Journal of Tribology*, vol. 127, no. 2, pp. 343–354, 2005. doi: 10.1115/1.1866166

[43] L. Kogut and I. Etsion, "Elastic-plastic contact analysis of a sphere and a rigid flat," *Journal of Applied Mechanics*, vol. 69, no. 5, pp. 657–662, 2002. doi: 10.1115/1.1490373

[44] S. L. Yan and L. Y. Li, "Finite element analysis of cyclic indentation of an elastic-perfectly plastic half-space by a rigid sphere," *Proceedings of the Institution of Mechanical Engineers Part C Journal of Mechanical Engeineering Science*, vol. 217, no. 5, pp. 505–514, 2003. doi: 10.1243/095440603765226795

[45] P. L. Larsson and E. Olsson, "A numerical study of the mechanical behavior at contact between particles of dissimilar elastic-ideally plastic materials," *Journal of Physics and Chemistry of Solids*, vol. 77, pp. 92–100, 2015. doi: 10.1016/j.jpcs.2014.08.016

[46] A. C. Rodríguez Urribarrí, E. van der Heide, X. Zeng, and M. B. de Rooij, "Modelling the static contact between a fingertip and a rigid wavy surface", *Tribology International*, vol. 102, pp. 114–124, 2016. doi: 10.1016/j.triboint.2016.05.028

[47] M. Danny Pratama Lamura, M. Imam Ammarullah, T. Hidayat, M. Izzur Maula, J. Jamari, and A. P. Bayuseno, "Diameter ratio and friction coefficient effect on equivalent plastic strain (PEEQ) during contact between two brass solids", *Cogent Engineering*, vol. 10, no. 1, pp. 1–7, 2023. doi: 10.1080/23311916.2023.2218691

[48] V. Saikko, "Analysis of wear produced by a 100-station wear test device for UHMWPE with different contact pressures", *Tribology International*, vol. 171, p. 107560, 2022. doi: 10.1016/j.triboint.2022.107560

[49] J. Burbank and M. Woydt, "Optimization of pre-conditioned cold work hardening of steel alloys for friction and wear reductions under slip-rolling contact", *Wear*, vol. 350–351, pp. 141–154, 2016. doi: 10.1016/j.wear.2016.01.011

[50] J. Jamari and D. J. Schipper, "Deterministic repeated contact of rough surfaces", *Wear*, vol. 264, no. 3–4, pp. 349–358, 2008. doi: 10.1016/j.wear.2007.03.024

[51] J. Jamari, R. Ismail, E. Saputra, S. Sugiyanto, and I. B. Anwar, "The effect of repeated impingement on UHMWPE material in artificial hip joint during salat activities," *Advanced Materials Research*, vo. 896, pp. 272–275, 2014. doi: 10.4028/www.scientific.net/AMR.896.272

[52] J. Jamari and D. J. Schipper, "Plastic deformation and contact area of an elastic-plastic contact of ellipsoid bodies after unloading," *Tribology International*, vol. 40, no. 8, pp. 1311–1318, 2007. doi: 10.1016/j.triboint.2007.02.015